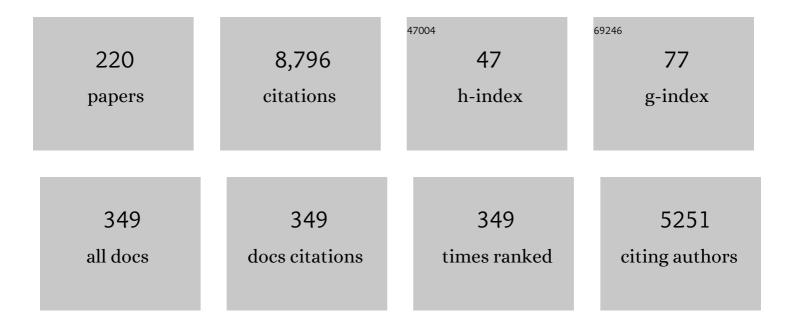
Kimberly Strong

List of Publications by Year in descending order

Source: https://exaly.com/author-pdf/2369163/publications.pdf Version: 2024-02-01



#	Article	IF	CITATIONS
1	Atmospheric Chemistry Experiment (ACE): Mission overview. Geophysical Research Letters, 2005, 32, .	4.0	768
2	An overview of the Odin atmospheric mission. Canadian Journal of Physics, 2002, 80, 309-319.	1.1	403
3	The OSIRIS instrument on the Odin spacecraft. Canadian Journal of Physics, 2004, 82, 411-422.	1.1	349
4	A method for evaluating bias in global measurements of CO ₂ total columns from space. Atmospheric Chemistry and Physics, 2011, 11, 12317-12337.	4.9	279
5	Improvement of the retrieval algorithm for GOSAT SWIR XCO ₂ and XCH ₄ and their validation using TCCON data. Atmospheric Measurement Techniques, 2013, 6, 1533-1547.	3.1	261
6	Comparisons of the Orbiting Carbon Observatory-2 (OCO-2) <i>X</i> _{CO₂&ar measurements with TCCON. Atmospheric Measurement Techniques, 2017, 10, 2209-2238.}	np; 8t;1 /sub8	&an ap ,gt;
7	Source attribution and interannual variability of Arctic pollution in spring constrained by aircraft (ARCTAS, ARCPAC) and satellite (AIRS) observations of carbon monoxide. Atmospheric Chemistry and Physics, 2010, 10, 977-996.	4.9	189
8	Improved retrievals of carbon dioxide from Orbiting Carbon Observatory-2 with the version 8 ACOS algorithm. Atmospheric Measurement Techniques, 2018, 11, 6539-6576.	3.1	188
9	Ground-based validation of the Copernicus Sentinel-5P TROPOMI NO ₂ measurements with the NDACC ZSL-DOAS, MAX-DOAS and Pandonia global networks. Atmospheric Measurement Techniques, 2021, 14, 481-510.	3.1	142
10	Validation of ozone measurements from the Atmospheric Chemistry Experiment (ACE). Atmospheric Chemistry and Physics, 2009, 9, 287-343.	4.9	134
11	Inferring regional sources and sinks of atmospheric CO ₂ from GOSAT XCO ₂ data. Atmospheric Chemistry and Physics, 2014, 14, 3703-3727.	4.9	120
12	Processâ€evaluation of tropospheric humidity simulated by general circulation models using water vapor isotopologues: 1. Comparison between models and observations. Journal of Geophysical Research, 2012, 117, .	3.3	114
13	CO measurements from the ACE-FTS satellite instrument: data analysis and validation using ground-based, airborne and spaceborne observations. Atmospheric Chemistry and Physics, 2008, 8, 2569-2594.	4.9	107
14	Intercomparison of slant column measurements of NO ₂ and O ₄ by MAX-DOAS and zenith-sky UV and visible spectrometers. Atmospheric Measurement Techniques, 2010, 3, 1629-1646.	3.1	106
15	Comparisons between SCIAMACHY and ground-based FTIR data for total columns of CO, CH ₄ , CO ₂ and N ₂ O. Atmospheric Chemistry and Physics, 2006, 6, 1953-1976.	4.9	103
16	Analysis of ozone and nitric acid in spring and summer Arctic pollution using aircraft, ground-based, satellite observations and MOZART-4 model: source attribution and partitioning. Atmospheric Chemistry and Physics, 2012, 12, 237-259.	4.9	96
17	Spectroscopic measurements of tropospheric CO, C2H6, C2H2, and HCN in northern Japan. Journal of Geophysical Research, 2002, 107, ACH 2-1.	3.3	95
18	Validation of ACE-FTS v2.2 measurements of HCl, HF, CCl ₃ F and CCl ₂ F ₂ using space-, balloon- and ground-based instrument observations. Atmospheric Chemistry and Physics, 2008, 8, 6199-6221.	4.9	91

#	Article	IF	CITATIONS
19	Validation of ACE-FTS v2.2 methane profiles from the upper troposphere to the lower mesosphere. Atmospheric Chemistry and Physics, 2008, 8, 2421-2435.	4.9	85
20	Global CO ₂ fluxes inferred from surface air-sample measurements and from TCCON retrievals of the CO ₂ total column. Geophysical Research Letters, 2011, 38, n/a-n/a.	4.0	85
21	Detection of stratospheric ozone intrusions by windprofiler radars. Nature, 2007, 450, 281-284.	27.8	84
22	Spectral parameters of self- and hydrogen-broadened methane from 2000 to 9500 cm-1 for remote sounding of the atmosphere of jupiter. Journal of Quantitative Spectroscopy and Radiative Transfer, 1993, 50, 363-429.	2.3	83
23	The Cabauw Intercomparison campaign for Nitrogen Dioxide measuring Instruments (CINDI): design, execution, and early results. Atmospheric Measurement Techniques, 2012, 5, 457-485.	3.1	83
24	Stratospheric ozone profiles retrieved from limb scattered sunlight radiance spectra measured by the OSIRIS instrument on the Odin satellite. Geophysical Research Letters, 2003, 30, .	4.0	82
25	Evaluating ethane and methane emissions associated with the development of oil and natural gas extraction in North America. Environmental Research Letters, 2016, 11, 044010.	5.2	82
26	Consistent evaluation of ACOS-GOSAT, BESD-SCIAMACHY, CarbonTracker, and MACC through comparisons to TCCON. Atmospheric Measurement Techniques, 2016, 9, 683-709.	3.1	80
27	MAX-DOAS formaldehyde slant column measurements during CINDI: intercomparison and analysis improvement. Atmospheric Measurement Techniques, 2013, 6, 167-185.	3.1	78
28	Validation of ACE-FTS N ₂ O measurements. Atmospheric Chemistry and Physics, 2008, 8, 4759-4786.	4.9	76
29	The high Arctic in extreme winters: vortex, temperature, and MLS and ACE-FTS trace gas evolution. Atmospheric Chemistry and Physics, 2008, 8, 505-522.	4.9	75
30	Validation of HNO ₃ , ClONO ₂ , and N ₂ O ₅ from the Atmospheric Chemistry Experiment Fourier Transform Spectrometer (ACE-FTS). Atmospheric Chemistry	4.9	75
31	and Physics, 2008, 8, 3529-3562. Observed and simulated time evolution of HCl, ClONO ₂ , and HF total column abundances. Atmospheric Chemistry and Physics, 2012, 12, 3527-3556.	4.9	72
32	A scientific algorithm to simultaneously retrieve carbon monoxide and methane from TROPOMI onboard Sentinel-5 Precursor. Atmospheric Measurement Techniques, 2019, 12, 6771-6802.	3.1	71
33	Ubiquitous atmospheric production of organic acids mediated by cloud droplets. Nature, 2021, 593, 233-237.	27.8	71
34	Ground-based remote sensing of tropospheric water vapour isotopologues within the project MUSICA. Atmospheric Measurement Techniques, 2012, 5, 3007-3027.	3.1	69
35	Assessment of the quality of TROPOMI high-spatial-resolution NO ₂ data products in the Greater Toronto Area. Atmospheric Measurement Techniques, 2020, 13, 2131-2159.	3.1	69
36	Validation of the Atmospheric Chemistry Experiment (ACE) version 2.2 temperature using ground-based and space-borne measurements. Atmospheric Chemistry and Physics, 2008, 8, 35-62.	4.9	68

#	Article	IF	CITATIONS
37	A New Bruker IFS 125HR FTIR Spectrometer for the Polar Environment Atmospheric Research Laboratory at Eureka, Nunavut, Canada: Measurements and Comparison with the Existing Bomem DA8 Spectrometer. Journal of Atmospheric and Oceanic Technology, 2009, 26, 1328-1340.	1.3	66
38	TROPOMI–Sentinel-5 Precursor formaldehyde validation using an extensive network of ground-based Fourier-transform infrared stations. Atmospheric Measurement Techniques, 2020, 13, 3751-3767.	3.1	66
39	Validation of NO ₂ and NO from the Atmospheric Chemistry Experiment (ACE). Atmospheric Chemistry and Physics, 2008, 8, 5801-5841.	4.9	64
40	Technical Note: New ground-based FTIR measurements at Ile de La Réunion: observations, error analysis, and comparisons with independent data. Atmospheric Chemistry and Physics, 2008, 8, 3483-3508.	4.9	61
41	Validation of methane and carbon monoxide from Sentinel-5 Precursor using TCCON and NDACC-IRWG stations. Atmospheric Measurement Techniques, 2021, 14, 6249-6304.	3.1	57
42	Stratospheric profiles of nitrogen dioxide observed by Optical Spectrograph and Infrared Imager System on the Odin satellite. Journal of Geophysical Research, 2003, 108, .	3.3	56
43	An evaluation of IASI-NH ₃ with ground-based Fourier transform infrared spectroscopy measurements. Atmospheric Chemistry and Physics, 2016, 16, 10351-10368.	4.9	56
44	Ground-Based Solar Absorption FTIR Spectroscopy: Characterization of Retrievals and First Results from a Novel Optical Design Instrument at a New NDACC Complementary Station. Journal of Atmospheric and Oceanic Technology, 2007, 24, 432-448.	1.3	55
45	A decade of GOSAT Proxy satellite CH ₄ observations. Earth System Science Data, 2020, 12, 3383-3412.	9.9	53
46	Quantifying the impact of BOReal forest fires on Tropospheric oxidants over the Atlantic using Aircraft and Satellites (BORTAS) experiment: design, execution and science overview. Atmospheric Chemistry and Physics, 2013, 13, 6239-6261.	4.9	52
47	Consistent regional fluxes of CH ₄ and CO ₂ inferred from GOSAT proxy XCH ₄ â€`:â€`XCO ₂ retrieva 2010–2014. Atmospheric Chemistry and Physics, 2017, 17, 4781-4797.	1 <mark>4.9</mark>	52
48	Validation of the CrIS fast physical NH ₃ retrieval with ground-based FTIR. Atmospheric Measurement Techniques, 2017, 10, 2645-2667.	3.1	52
49	Intercomparison of NO ₂ , O ₄ , O ₃ and HCHO slant column measurements by MAX-DOAS and zenith-sky UV–visible spectrometers during CINDI-2. Atmospheric Measurement Techniques. 2020. 13. 2169-2208.	3.1	52
50	COVIDâ€19 Crisis Reduces Free Tropospheric Ozone Across the Northern Hemisphere. Geophysical Research Letters, 2021, 48, e2020GL091987.	4.0	51
51	Midlatitude observations of the diurnal variation of stratospheric BrO. Journal of Geophysical Research, 1995, 100, 18863.	3.3	45
52	Longâ€range transport of NH ₃ , CO, HCN, and C ₂ H ₆ from the 2014 Canadian Wildfires. Geophysical Research Letters, 2016, 43, 8286-8297.	4.0	44
53	Validation of MOPITT carbon monoxide using ground-based Fourier transform infrared spectrometer data from NDACC. Atmospheric Measurement Techniques, 2017, 10, 1927-1956.	3.1	44
54	Measurements of O3, NO2and Temperature during the 2004 Canadian Arctic ACE Validation Campaign. Geophysical Research Letters, 2005, 32, .	4.0	43

#	Article	IF	CITATIONS
55	Revisiting global fossil fuel and biofuel emissions of ethane. Journal of Geophysical Research D: Atmospheres, 2017, 122, 2493-2512.	3.3	43
56	A performance assessment of the World Wide Lightning Location Network (WWLLN) via comparison with the Canadian Lightning Detection Network (CLDN). Atmospheric Measurement Techniques, 2010, 3, 1143-1153.	3.1	39
57	Using XCO ₂ retrievals for assessing the long-term consistency of NDACC/FTIR data sets. Atmospheric Measurement Techniques, 2015, 8, 1555-1573.	3.1	39
58	Tropospheric CH ₄ signals as observed by NDACC FTIR at globally distributed sites and comparison to GAW surface in situ measurements. Atmospheric Measurement Techniques, 2014, 7, 2337-2360.	3.1	38
59	A case study of a transported bromine explosion event in the Canadian high arctic. Journal of Geophysical Research D: Atmospheres, 2016, 121, 457-477.	3.3	38
60	New nitric oxide (NO) nightglow measurements with SPICAM/MEx as a tracer of Mars upper atmosphere circulation and comparison with LMDâ€MGCM model prediction: Evidence for asymmetric hemispheres. Journal of Geophysical Research E: Planets, 2013, 118, 2172-2179.	3.6	37
61	C ₂ H ₆ , C ₂ H ₂ , CH ₃ OH, HCOOH and H&:lt:sub>:2&:lt:/sub>CO total columns measured in the Canadian high Arctic.	3.1	37
62	Toward a chemical reanalysis in a coupled chemistryâ€climate model: An evaluation of MOPITT CO assimilation and its impact on tropospheric composition. Journal of Geophysical Research D: Atmospheres, 2016, 121, 7310-7343.	3.3	37
63	NDACC harmonized formaldehyde time series from 21 FTIR stations covering a wide range of column abundances. Atmospheric Measurement Techniques, 2018, 11, 5049-5073.	3.1	37
64	A coolable long path absorption cell for laboratory spectroscopic studies of gases. Journal of Quantitative Spectroscopy and Radiative Transfer, 1994, 52, 677-691.	2.3	35
65	Unusually low ozone, HCl, and HNO ₃ column measurements at Eureka, Canada during winter/spring 2011. Atmospheric Chemistry and Physics, 2012, 12, 3821-3835.	4.9	34
66	Global land mapping of satellite-observed CO ₂ total columns using spatio-temporal geostatistics. International Journal of Digital Earth, 2017, 10, 426-456.	3.9	33
67	The recent increase of atmospheric methane from 10 years of ground-based NDACC FTIR observations since 2005. Atmospheric Chemistry and Physics, 2017, 17, 2255-2277.	4.9	33
68	Intercomparison of MAX-DOAS vertical profile retrieval algorithms: studies on field data from the CINDI-2 campaign. Atmospheric Measurement Techniques, 2021, 14, 1-35.	3.1	32
69	Ammonia and PM2.5 Air Pollution in Paris during the 2020 COVID Lockdown. Atmosphere, 2021, 12, 160.	2.3	32
70	Polar vortex evolution during the 2002 Antarctic major warming as observed by the Odin satellite. Journal of Geophysical Research, 2005, 110, .	3.3	31
71	Technical Note: Validation of Odin/SMR limb observations of ozone, comparisons with OSIRIS, POAM III, ground-based and balloon-borne instruments. Atmospheric Chemistry and Physics, 2008, 8, 3385-3409.	4.9	31
72	Severe 2011 ozone depletion assessed with 11 years of ozone, NO ₂ , and OClO measurements at 80ŰN. Geophysical Research Letters, 2012, 39, .	4.0	30

#	Article	IF	CITATIONS
73	An exemplary case of a bromine explosion event linked to cyclone development in the Arctic. Atmospheric Chemistry and Physics, 2016, 16, 1773-1788.	4.9	29
74	Comparisons between ACE-FTS and ground-based measurements of stratospheric HCl and ClONO2loadings at northern latitudes. Geophysical Research Letters, 2005, 32, .	4.0	28
75	OSIRIS: A Decade of Scattered Light. Bulletin of the American Meteorological Society, 2012, 93, 1845-1863.	3.3	28
76	Validation of ACE and OSIRIS ozone and NO ₂ measurements using ground-based instruments at 80° N. Atmospheric Measurement Techniques, 2012, 5, 927-953.	3.1	28
77	Identifying fire plumes in the Arctic with tropospheric FTIR measurements and transport models. Atmospheric Chemistry and Physics, 2015, 15, 2227-2246.	4.9	28
78	Seasonal variations of HCN over northern Japan measured by ground-based infrared solar spectroscopy. Geophysical Research Letters, 2000, 27, 2085-2088.	4.0	27
79	Simultaneous ground-based observations of O ₃ , HCl, N ₂ O, and CH ₄ over Toronto, Canada by three Fourier transform spectrometers with different resolutions. Atmospheric Chemistry and Physics. 2007. 7. 1275-1292.	4.9	27
80	Characterizing model errors in chemical transport modeling of methane: impact of model resolution in versions v9-02 of GEOS-Chem and v35j of its adjoint model. Geoscientific Model Development, 2020, 13, 3839-3862.	3.6	27
81	Occurrence of weak, subâ€micron, tropospheric aerosol events at high Arctic latitudes. Geophysical Research Letters, 2008, 35, .	4.0	26
82	Improved Constraints on Northern Extratropical CO ₂ Fluxes Obtained by Combining Surfaceâ€Based and Spaceâ€Based Atmospheric CO ₂ Measurements. Journal of Geophysical Research D: Atmospheres, 2020, 125, e2019JD032029.	3.3	26
83	Detection and attribution of wildfire pollution in the Arctic and northern midlatitudes using a network of Fourier-transform infrared spectrometers and GEOS-Chem. Atmospheric Chemistry and Physics, 2020, 20, 12813-12851.	4.9	26
84	Tropospheric water vapour isotopologue data (H ₂ ¹⁶ O,) Tj ETQq0 0 0 r	gBT /Over 9.9	lock 10 Tf 50 26
85	Earth System Science Data, 2017, 9, 15-29. Zenith-sky observations of stratospheric gases: the sensitivity of air mass factors to geophysical parameters and the influence of tropospheric clouds. Journal of Quantitative Spectroscopy and Radiative Transfer, 2001, 68, 657-677.	2.3	25
86	MANTRA ―A Balloon Mission to Study the Oddâ€Nitrogen Budget of the Stratosphere. Atmosphere - Ocean, 2005, 43, 283-299.	1.6	25
87	Technical Note: Latitude-time variations of atmospheric column-average dry air mole fractions of CO ₂ , CH ₄ and N ₂ O. Atmospheric Chemistry and Physics, 2012, 12, 7767-7777.	4.9	25
88	Unprecedented Atmospheric Ammonia Concentrations Detected in the High Arctic From the 2017 Canadian Wildfires. Journal of Geophysical Research D: Atmospheres, 2019, 124, 8178-8202.	3.3	25
89	Temperature dependence of self- and N2-broadeningand pressure-induced shifts in the 3â†0 band of CO. Journal of Molecular Structure, 2004, 695-696, 269-286.	3.6	24
90	An evaluation of infrared microwindows for ozone retrievals using the Eureka Bruker 125HR Fourier transform spectrometer. Journal of Quantitative Spectroscopy and Radiative Transfer, 2010, 111, 569-585.	2.3	24

#	Article	IF	CITATIONS
91	Infrared measurements in the Arctic using two Atmospheric Emitted Radiance Interferometers. Atmospheric Measurement Techniques, 2012, 5, 329-344.	3.1	24
92	Sensitivity of CO ₂ surface flux constraints to observational coverage. Journal of Geophysical Research D: Atmospheres, 2017, 122, 6672-6694.	3.3	24
93	Odin observations of Antarctic nighttime NO densities in the mesosphere–lower thermosphere and observations of a lower NO layer. Journal of Geophysical Research D: Atmospheres, 2013, 118, 7414-7425.	3.3	23
94	The impact of the OSIRIS grating efficiency on radiance and trace-gas retrievals. Canadian Journal of Physics, 2002, 80, 469-481.	1.1	22
95	First measurements of <mml:math <br="" altimg="si53.gif" xmlns:mml="http://www.w3.org/1998/Math/Math/L">overflow="scroll"><mml:msub><mml:mrow><mml:mi mathvariant="normal">O</mml:mi </mml:mrow><mml:mrow><mml:mn>3</mml:mn></mml:mrow><mml:math <="" altimg="si54.gif" td="" xmlns:mml="http://www.w3.org/1998/Math/MathML"><td>>^{2.3}/mml:m</td><td>ath>,</td></mml:math></mml:msub></mml:math>	> ^{2.3} /mml:m	ath>,
96	overflow="scroll"> <mml:msub><mml:mrow><mml:mi>NO</mml:mi><mml:mrow><mml:mrow><mml:mn>2Recent Arctic ozone depletion: Is there an impact of climate change?. Comptes Rendus - Geoscience, 2018, 350, 347-353.</mml:mn></mml:mrow></mml:mrow></mml:mrow></mml:msub>	nl:mn> <. 1.2	22
97	Ensemble-based satellite-derived carbon dioxide and methane column-averaged dry-air mole fraction data sets (2003–2018) for carbon and climate applications. Atmospheric Measurement Techniques, 2020, 13, 789-819.	3.1	22
98	Evaluating GPP and Respiration Estimates Over Northern Midlatitude Ecosystems Using Solarâ€Induced Fluorescence and Atmospheric CO ₂ Measurements. Journal of Geophysical Research G: Biogeosciences, 2018, 123, 2976-2997.	3.0	21
99	Evaluation of MOPITT VersionÂ7 joint TIR–NIR X _{CO} retrievals with TCCON. Atmospheric Measurement Techniques, 2019, 12, 5547-5572.	3.1	21
100	Spaceborne Measurements of Formic and Acetic Acids: A Global View of the Regional Sources. Geophysical Research Letters, 2020, 47, e2019GL086239.	4.0	21
101	Visible intracavity laser spectroscopy with a step-scan Fourier-transform interferometer. Applied Optics, 1997, 36, 8533.	2.1	20
102	Retrieval of vertical concentration profiles from OSIRIS UV—visible limb spectra. Canadian Journal of Physics, 2002, 80, 409-434.	1.1	20
103	Nighttime nitric oxide densities in the Southern Hemisphere mesosphere–lower thermosphere. Geophysical Research Letters, 2011, 38, .	4.0	20
104	Towards understanding the variability in biospheric CO ₂ Âfluxes: using FTIR spectrometry and a chemical transport model to investigate the sources and sinks of carbonyl sulfide and its link to CO ₂ . Atmospheric Chemistry and Physics, 2016, 16, 2123-2138.	4.9	20
105	Investigating differences in DOAS retrieval codes using MAD-CAT campaign data. Atmospheric Measurement Techniques, 2017, 10, 955-978.	3.1	20
106	Characterization of aerosol growth events over Ellesmere Island during the summers of 2015 and 2016. Atmospheric Chemistry and Physics, 2019, 19, 5589-5604.	4.9	20
107	Using a speed-dependent Voigt line shape to retrieve O ₂ from Total Carbon Column Observing Network solar spectra to improve measurements of XCO ₂ . Atmospheric Measurement Techniques, 2019, 12, 35-50.	3.1	20
108	Gas phase UV and IR absorption spectra of CF3CH2CH2OH and F(CF2CF2)xCH2CH2OH (x=2, 3, 4). Journal of Fluorine Chemistry, 2005, 126, 1288-1296.	1.7	19

#	Article	IF	CITATIONS
109	Modeled O ₂ nightglow distributions in the Venusian atmosphere. Journal of Geophysical Research, 2012, 117, .	3.3	19
110	Measurements of CO, HCN, and C ₂ H ₆ Total Columns in Smoke Plumes Transported from the 2010 Russian Boreal Forest Fires to the Canadian High Arctic. Atmosphere - Ocean, 2013, 51, 522-531.	1.6	19
111	Climatology and predictability of the late summer stratospheric zonal wind turnaround over Vanscoy, Saskatchewan. Atmosphere - Ocean, 2005, 43, 301-313.	1.6	18
112	Intercomparison of UV-visible measurements of ozone and NO ₂ during the Canadian Arctic ACE validation campaigns: 2004–2006. Atmospheric Chemistry and Physics, 2008, 8, 1763-1788.	4.9	17
113	A global inventory of stratospheric NO _{<i>y</i>} from ACE-FTS. Journal of Geophysical Research, 2011, 116, .	3.3	17
114	Greenhouse gas simulations with a coupled meteorological and transport model: the predictability of CO ₂ . Atmospheric Chemistry and Physics, 2016, 16, 12005-12038.	4.9	17
115	Fourier transform infrared time series of tropospheric HCN in eastern China: seasonality, interannual variability, and source attribution. Atmospheric Chemistry and Physics, 2020, 20, 5437-5456.	4.9	17
116	An 11-year record of XCO ₂ estimates derived from GOSAT measurements using the NASA ACOS version 9 retrieval algorithm. Earth System Science Data, 2022, 14, 325-360.	9.9	17
117	Groundâ€based measurements of ozone and NO2during MANTRA 1998 using a Zenithâ€sky spectrometer. Atmosphere - Ocean, 2005, 43, 325-338.	1.6	16
118	Investigation of CO, C ₂ H ₆ and aerosols in a boreal fire plume over eastern Canada during BORTAS 2011 using ground- and satellite-based observations and model simulations. Atmospheric Chemistry and Physics, 2013, 13, 10227-10241.	4.9	16
119	Intercomparison of atmospheric water vapour measurements at a Canadian High Arctic site. Atmospheric Measurement Techniques, 2017, 10, 2851-2880.	3.1	16
120	Four Fourier transform spectrometers and the Arctic polar vortex: instrument intercomparison and ACE-FTS validation at Eureka during the IPY springs of 2007 and 2008. Atmospheric Measurement Techniques, 2010, 3, 51-66.	3.1	16
121	Temperature-dependent absorption cross-sections of HCFC-142b. Journal of Quantitative Spectroscopy and Radiative Transfer, 2010, 111, 364-371.	2.3	15
122	OH Meinel band nightglow profiles from OSIRIS observations. Journal of Geophysical Research D: Atmospheres, 2014, 119, 11,417.	3.3	15
123	Toronto area ozone: Longâ€ŧerm measurements and modeled sources of poor air quality events. Journal of Geophysical Research D: Atmospheres, 2015, 120, 11,368.	3.3	15
124	Mid-infrared absorption cross-sections and temperature dependence of CFC-113. Journal of Quantitative Spectroscopy and Radiative Transfer, 2011, 112, 1280-1285.	2.3	14
125	The Atmospheric Imaging Mission for Northern Regions: AIM-North. Canadian Journal of Remote Sensing, 2019, 45, 423-442.	2.4	14
126	Retrieval of atmospheric CO ₂ vertical profiles from ground-based near-infrared spectra. Atmospheric Measurement Techniques, 2021, 14, 3087-3118.	3.1	14

#	Article	IF	CITATIONS
127	Characterizing model errors in chemical transport modeling of methane: using GOSAT XCH ₄ data with weak-constraint four-dimensional variational data assimilation. Atmospheric Chemistry and Physics, 2021, 21, 9545-9572.	4.9	14
128	Pan-Arctic surface ozone: modelling vs. measurements. Atmospheric Chemistry and Physics, 2020, 20, 15937-15967.	4.9	14
129	Estimating biases and error variances through the comparison of coincident satellite measurements. Journal of Geophysical Research, 2007, 112, .	3.3	13
130	Validating the reported random errors of ACEâ€FTS measurements. Journal of Geophysical Research, 2010, 115, .	3.3	13
131	Assessment of the quality of OSIRIS mesospheric temperatures using satellite and ground-based measurements. Atmospheric Measurement Techniques, 2012, 5, 2993-3006.	3.1	13
132	The spring 2011 final stratospheric warming above Eureka: anomalous dynamics and chemistry. Atmospheric Chemistry and Physics, 2013, 13, 611-624.	4.9	13
133	On what scales can GOSAT flux inversions constrain anomalies in terrestrial ecosystems?. Atmospheric Chemistry and Physics, 2019, 19, 13017-13035.	4.9	13
134	Scanning the Earth's Limb from a High-Altitude Balloon: The Development and Flight of a New Balloon-Based Pointing System. Journal of Atmospheric and Oceanic Technology, 2002, 19, 618-632.	1.3	12
135	A method for recovering stratospheric minor species densities from the Odin/OSIRIS scattered-sunlight measurements. Canadian Journal of Physics, 2002, 80, 395-408.	1.1	12
136	Nitric acid measurements at Eureka obtained in winter 2001–2002 using solar and lunar Fourier transform infrared absorption spectroscopy: Comparisons with observations at Thule and Kiruna and with results from three-dimensional models. Journal of Geophysical Research, 2007, 112, .	3.3	12
137	Comparison of the CMAM30 data set with ACE-FTS and OSIRIS: polar regions. Atmospheric Chemistry and Physics, 2015, 15, 12465-12485.	4.9	12
138	Methane cross-validation between three Fourier transform spectrometers: SCISAT ACE-FTS, GOSAT TANSO-FTS, and ground-based FTS measurements in the Canadian high Arctic. Atmospheric Measurement Techniques, 2016, 9, 1961-1980.	3.1	12
139	Temperature-dependent absorption cross-sections of perfluorotributylamine. Journal of Molecular Spectroscopy, 2016, 323, 53-58.	1.2	12
140	Atmospheric Implications of Large C ₂ â€C ₅ Alkane Emissions From the U.S. Oil and Gas Industry. Journal of Geophysical Research D: Atmospheres, 2019, 124, 1148-1169.	3.3	12
141	Accuracy, precision, and temperature dependence of Pandora total ozone measurements estimated from a comparison with the Brewer triad in Toronto. Atmospheric Measurement Techniques, 2016, 9, 5747-5761.	3.1	12
142	Global Atmospheric OCS Trend Analysis From 22 NDACC Stations. Journal of Geophysical Research D: Atmospheres, 2022, 127, .	3.3	12
143	First detection of meso-thermospheric Nitric Oxide (NO) by ground-based FTIR solar absorption spectroscopy. Geophysical Research Letters, 2006, 33, .	4.0	11
144	Summertime stratospheric processes at northern mid-latitudes: comparisons between MANTRA balloon measurements and the Canadian Middle Atmosphere Model. Atmospheric Chemistry and Physics, 2008, 8, 2057-2071.	4.9	11

#	Article	IF	CITATIONS
145	Measurements of the infrared absorption cross-sections of HCFC-141b (CH3CFCl2). Journal of Quantitative Spectroscopy and Radiative Transfer, 2012, 113, 1913-1919.	2.3	11
146	Mars methane analogue mission: Mission simulation and rover operations at Jeffrey Mine and Norbestos Mine Quebec, Canada. Advances in Space Research, 2015, 55, 2414-2426.	2.6	11
147	Cyclone-induced surface ozone and HDO depletion in the Arctic. Atmospheric Chemistry and Physics, 2017, 17, 14955-14974.	4.9	11
148	Updated validation of ACE and OSIRIS ozone and NO2 measurements in the Arctic using ground-based instruments at Eureka, Canada. Journal of Quantitative Spectroscopy and Radiative Transfer, 2019, 238, 106571.	2.3	11
149	Evaluating different methods for elevation calibration of MAX-DOAS (Multi AXis Differential Optical) Tj ETQq1 1 Techniques, 2020, 13, 685-712.	0.784314 3.1	rgBT /Overloo 11
150	Remote measurements of vertical profiles of atmospheric constituents with a UV–visible ranging spectrometer. Applied Optics, 1995, 34, 6223.	2.1	10
151	Improving atmospheric CO2 retrievals using line mixing and speed-dependence when fitting high-resolution ground-based solar spectra. Journal of Molecular Spectroscopy, 2016, 323, 15-27.	1.2	10
152	Conformational analysis and global warming potentials of 1,1,1,3,3,3-hexafluoro-2-propanol from absorption spectroscopy. Journal of Quantitative Spectroscopy and Radiative Transfer, 2017, 203, 522-529.	2.3	10
153	A study of the temperature dependence of the infrared absorption cross-sections of 2,2,3,3,3-pentafluoropropanol in the range of 298–362 K. Journal of Quantitative Spectroscopy and Radiative Transfer, 2017, 186, 150-157.	2.3	10
154	Study of the footprints of short-term variation in XCO ₂ observed by TCCON sites using NIES and FLEXPART atmospheric transport models. Atmospheric Chemistry and Physics, 2017, 17, 143-157.	4.9	10
155	Comparison of the GOSAT TANSO-FTS TIR CH ₄ volume mixing ratio vertical profiles with those measured by ACE-FTS, ESA MIPAS, IMK-IAA MIPAS, and 16 NDACC stations. Atmospheric Measurement Techniques, 2017, 10, 3697-3718.	3.1	10
156	Monitoring Urban Greenhouse Gases Using Open-Path Fourier Transform Spectroscopy. Atmosphere - Ocean, 2020, 58, 25-45.	1.6	10
157	Retrieval of greenhouse gases from GOSAT and GOSAT-2 using the FOCAL algorithm. Atmospheric Measurement Techniques, 2022, 15, 3401-3437.	3.1	10
158	An extended intercomparison of simultaneous ground-based Fourier transform infrared spectrometer measurements at the Toronto Atmospheric Observatory. Journal of Quantitative Spectroscopy and Radiative Transfer, 2008, 109, 2244-2260.	2.3	9
159	Simultaneous trace gas measurements using two Fourier transform spectrometers at Eureka, Canada during spring 2006, and comparisons with the ACE-FTS. Atmospheric Chemistry and Physics, 2011, 11, 5383-5405.	4.9	9
160	Using high-resolution laboratory and ground-based solar spectra to assess CH4 absorption coefficient calculations. Journal of Quantitative Spectroscopy and Radiative Transfer, 2017, 190, 48-59.	2.3	9
161	Multi-year comparisons of ground-based and space-borne Fourier transform spectrometers in the high Arctic between 2006 and 2013. Atmospheric Measurement Techniques, 2017, 10, 3273-3294.	3.1	9
162	Characterization and potential for reducing optical resonances in Fourier transform infrared spectrometers of the Network for the Detection of Atmospheric Composition Change (NDACC). Atmospheric Measurement Techniques, 2021, 14, 1239-1252.	3.1	9

#	Article	IF	CITATIONS
163	Ozone and NO ₂ variations measured during the 1 August 2008 solar eclipse above Eureka, Canada with a UVâ€visible spectrometer. Journal of Geophysical Research, 2010, 115, .	3.3	8
164	A study of the Arctic NOybudget above Eureka, Canada. Journal of Geophysical Research, 2011, 116, n/a-n/a.	3.3	8
165	Modeled O ₂ airglow distributions in the Martian atmosphere. Journal of Geophysical Research, 2012, 117, .	3.3	8
166	Infrared absorption cross-sections, radiative efficiency and global warming potential of HFC-43-10mee. Journal of Molecular Spectroscopy, 2018, 348, 64-67.	1.2	8
167	Collisionâ€Induced Absorption of CH ₄ â€CO ₂ and H ₂ â€CO ₂ Complexes and Their Effect on the Ancient Martian Atmosphere. Journal of Geophysical Research E: Planets, 2020, 125, e2019JE006357.	3.6	8
168	Measurements of Tropospheric Bromine Monoxide Over Four Halogen Activation Seasons in the Canadian High Arctic. Journal of Geophysical Research D: Atmospheres, 2020, 125, e2020JD033015.	3.3	8
169	Detection of HCOOH, CH ₃ OH, CO, HCN, and C ₂ H ₆ in Wildfire Plumes Transported Over Toronto Using Groundâ€Based FTIR Measurements From 2002–2018. Journal of Geophysical Research D: Atmospheres, 2020, 125, e2019JD031924.	3.3	8
170	NO2 vertical profiles retrieved from ground-based measurements during spring 1999 in the Canadian Arctic. Advances in Space Research, 2004, 34, 786-792.	2.6	7
171	Using airglow measurements to observe gravity waves in the Martian atmosphere. Advances in Space Research, 2006, 38, 730-738.	2.6	7
172	Intercomparison of ground-based ozone and NO ₂ measurements during the MANTRA 2004 campaign. Atmospheric Chemistry and Physics, 2007, 7, 5489-5499.	4.9	7
173	Lightning-produced NO ₂ observed by two ground-based UV-visible spectrometers at Vanscoy, Saskatchewan in August 2004. Atmospheric Chemistry and Physics, 2007, 7, 1683-1692.	4.9	7
174	Structure and conformational analysis of CFC-113 by density functional theory calculations and FTIR spectroscopy. Journal of Molecular Spectroscopy, 2007, 243, 142-147.	1.2	7
175	Assessing the impact of clouds on ground-based UV–visible total column ozone measurements in the high Arctic. Atmospheric Measurement Techniques, 2019, 12, 2463-2483.	3.1	7
176	First retrievals of peroxyacetyl nitrate (PAN) from ground-based FTIR solar spectra recorded at remote sites, comparison with model and satellite data. Elementa, 2021, 9, .	3.2	7
177	Multiscale observations of NH ₃ around Toronto, Canada. Atmospheric Measurement Techniques, 2021, 14, 905-921.	3.1	7
178	Unprecedented Spring 2020 Ozone Depletion in the Context of 20ÂYears of Measurements at Eureka, Canada. Journal of Geophysical Research D: Atmospheres, 2021, 126, e2020JD034365.	3.3	7
179	Tropospheric and Surface Nitrogen Dioxide Changes in the Greater Toronto Area during the First Two Years of the COVID-19 Pandemic. Remote Sensing, 2022, 14, 1625.	4.0	7
180	Automated ground-based star-pointing UV–visible spectrometer for stratospheric measurements. Applied Optics, 1997, 36, 6069.	2.1	6

#	Article	IF	CITATIONS
181	Retrieval of stratospheric NO2vertical profiles from groundâ€based zenithâ€sky DOAS measurements: Results for the MANTRA 1998 field campaign. Atmosphere - Ocean, 2005, 43, 339-350.	1.6	6
182	Year-round retrievals of trace gases in the Arctic using the Extended-range Atmospheric Emitted Radiance Interferometer. Atmospheric Measurement Techniques, 2013, 6, 1549-1565.	3.1	6
183	Using FTIR measurements of stratospheric composition to identify midlatitude polar vortex intrusions over Toronto. Journal of Geophysical Research D: Atmospheres, 2013, 118, 12,766.	3.3	6
184	The concentration profile of nitric acid and other species over Saskatchewan in August 1998: Retrieval from data recorded by thermalâ€emission radiometry. Atmosphere - Ocean, 2005, 43, 361-376.	1.6	5
185	Comparison of OSIRIS stratospheric NO2 and O3 measurements with ground-based Fourier transform spectrometer measurements at the Toronto Atmospheric Observatory. Canadian Journal of Physics, 2007, 85, 1301-1316.	1.1	5
186	Radiative efficiency and global warming potential of the hydrofluoroether HFE-356mec3 (CH3OCF2CHFCF3) from experimental and theoretical infrared absorption cross-sections. Journal of Molecular Spectroscopy, 2020, 367, 111241.	1.2	5
187	Quantifying the Impact of the COVID-19 Pandemic Restrictions on CO, CO2, and CH4 in Downtown Toronto Using Open-Path Fourier Transform Spectroscopy. Atmosphere, 2021, 12, 848.	2.3	5
188	The Adaptable 4A Inversion (5AI): description and first <i>X</i> _{CO₂&an retrievals from Orbiting Carbon Observatory-2 (OCO-2) observations. Atmospheric Measurement Techniques, 2021, 14, 4689-4706.}	np;]t;/sub8	amp;gt;
189	Smallâ€scale methane dispersion modelling for possible plume sources on the surface of Mars. Geophysical Research Letters, 2012, 39, .	4.0	4
190	Comparison of ground-based and satellite measurements of water vapour vertical profiles over Ellesmere Island, Nunavut. Atmospheric Measurement Techniques, 2019, 12, 4039-4063.	3.1	4
191	Assessing the feasibility of using a neural network to filter Orbiting Carbon ObservatoryÂ2 (OCO-2) retrievals at northern high latitudes. Atmospheric Measurement Techniques, 2021, 14, 7511-7524.	3.1	4
192	Application of the Fröhlich theory to the modelling of rouleau formation in human erythrocytes. Journal of Biological Physics, 1989, 17, 19-40.	1.5	3
193	Balloon-borne radiometer measurements of Northern Hemisphere mid-latitude stratospheric HNO ₃ profiles spanning 12 years. Atmospheric Chemistry and Physics, 2007, 7, 6075-6084.	4.9	3
194	Effects of vertical grid discretization in infrared transmission modeling. Journal of Quantitative Spectroscopy and Radiative Transfer, 2008, 109, 2463-2490.	2.3	3
195	New temperature and pressure retrieval algorithm for high-resolution infrared solar occultation spectroscopy: analysis and validation against ACE-FTS and COSMIC. Atmospheric Measurement Techniques, 2016, 9, 1063-1082.	3.1	3
196	Cis- and trans-perfluorodecalin: Infrared spectra, radiative efficiency and global warming potential. Journal of Quantitative Spectroscopy and Radiative Transfer, 2017, 203, 538-541.	2.3	3
197	Conformational analysis and global warming potentials of 1,1,1,2,3,3-hexafluoropropane and 1,1,2,2,3-pentafluoropropane from absorption spectroscopy. Journal of Quantitative Spectroscopy and Radiative Transfer, 2019, 225, 337-350.	2.3	2
198	Measurements of stratospheric composition in the Canadian Arctic during spring 1999-2002 using a UV-visible spectrometer. , 0, , .		1

#	Article	IF	CITATIONS
199	Retrieval of stratospheric NO/sub 2/ vertical profiles from ground-based measurements at Vanscoy, Saskatchewan. , 0, , .		1
200	Arctic Surface Properties and Their Impact on Microwave Satellite Water Vapor Column Retrievals. IEEE Transactions on Geoscience and Remote Sensing, 2020, 58, 8332-8344.	6.3	1
201	Atmospheric trace gas trends obtained from FTIR column measurements in Toronto, Canada from 2002-2019. Environmental Research Communications, 2021, 3, 051002.	2.3	1
202	Absorption cross-sections, radiative efficiency and global warming potential of HFE-347pcf2 (1,1,2,2-tetrafluoroethyl 2,2,2-trifluoroethyl ether). Journal of Molecular Spectroscopy, 2021, 379, 111494.	1.2	1
203	Trace Gases in the Arctic Atmosphere. Springer Polar Sciences, 2020, , 153-207.	0.1	1
204	Intercomparison of CO measurements from TROPOMI, ACE-FTS, and a high-Arctic ground-based Fourier transform spectrometer. Atmospheric Measurement Techniques, 2021, 14, 7707-7728.	3.1	1
205	Visible intracavity laser spectroscopy with a step-scan FTIR. , 1998, , .		0
206	A new high-resolution Fourier transform infrared spectrometer for ground-based atmospheric measurements in Toronto. , 0, , .		0
207	Temperature and pressure retrievals from the MAESTRO space instrument. , 0, , .		0
208	Ground-based Fourier-transform infrared measurements of atmospheric trace gases over Toronto, Canada. , 0, , .		0
209	Relative enhancements of ozone, carbon monoxide, nitrogen dioxide, and aerosols at the Earth's surface during Asian dust episodes in spring. , 0, , .		0
210	A Canadian atmospheric and geological mission to Mars. , 0, , .		0
211	Mechanism for Asian dust transport during blocking episode days in east Asia and North America in spring 2001. , 0, , .		0
212	The MANTRA campaigns - studying the stratosphere from balloons. , 0, , .		0
213	Corrigendum to "Lightning-produced NO ₂ observed by two ground-based UV-visible spectrometers at Vanscoy, Saskatchewan in August 2004" published in Atmos. Chem. Phys., 7, 1683–1692, 2007. Atmospheric Chemistry and Physics, 2008, 8, 5521-5523.	4.9	0
214	Infrared measurements throughout polar night using two AERIs in the Arctic. Proceedings of SPIE, 2012, , .	0.8	0
215	Simulation of source intensity variations from atmospheric dust for solar occultation Fourier transform infrared spectroscopy at Mars. Journal of Molecular Spectroscopy, 2016, 323, 78-85.	1.2	0
216	Distributions of Downwelling Radiance at 10 and 20 μm in the High Arctic. Atmosphere - Ocean, 2016, 54, 529-540.	1.6	0

#	Article	IF	CITATIONS
217	The NOy Budget Above Eureka, Nunavut From Ground-based FTIR Measurements, Space-based ACE-FTS Measurements, and the CMAM-DAS, GEM-BACH, and SLIMCAT Models. , 2011, , .		ο
218	Probing Atmospheric Composition over Canada using Ground-based FTIR Spectroscopy. , 2013, , .		0
219	Nitrous Oxide Profiling from Infrared Radiances (NOPIR): Algorithm Description, Application to 10 Years of IASI Observations and Quality Assessment. Remote Sensing, 2022, 14, 1810.	4.0	Ο
220	Ground-based validation of the MetOp-A and MetOp-B GOME-2 OClO measurements. Atmospheric Measurement Techniques, 2022, 15, 3439-3463.	3.1	0